Measurement report: Exploring the $NH_3$ behaviors at urban and suburban Beijing: Comparison and implications

Ziru Lan[a], Weili Lin[a], Weiwei Pu[b], Zhiqiang Ma[b,c]

[a]College of Life and Environmental Sciences, Minzu University of China, Beijing 100081;

[b]Environmental Meteorological Forecast Center of Beijing-Tianjin-Hebei, Beijing, 100089, China;

[c]Beijing Shangdianzi Regional Atmosphere Watch Station, Beijing, 101507, China

Correspondence: Weili Lin (linwl@muc.edu.cn)

**ABSTRACT**

Ammonia ($NH_3$) plays an important role in particulate matter formation; however, few long-term observations with a high temporal resolution have been conducted on the $NH_3$ concentrations in Beijing. In this study, online ammonia analyzers were used to observe continuously the atmospheric $NH_3$ concentrations at an urban site and a suburban site in Beijing from January 13, 2018, to January 13, 2019. The average mixing ratio of $NH_3$ at the urban site was 21 ± 14 ppb (range: 1.6–133 ppb) and that at the suburban site was 22 ± 15 ppb (range: 0.8–199 ppb). The $NH_3$ mixing ratios at the urban and suburban sites exhibited similar seasonal variations, with high values being observed in the summer and spring and low values being observed in the autumn and winter. The hourly mean $NH_3$ mixing ratios at the urban site were highly correlated ($R = 0.849$, $P < 0.01$) with those at the suburban site. However, the average diurnal variations in the $NH_3$ mixing ratios at the urban and suburban sites differed significantly, which indicated the different contributions of $NH_3$ sources and sinks at the urban and suburban sites. In addition to the emission sources, meteorological factors were closely related to the changes in the $NH_3$ concentrations. For the same temperature (relative humidity) at the urban and suburban sites, the $NH_3$ mixing ratios increased with the relative humidity (temperature). The relative humidity was the factor with the strongest influence on the $NH_3$ mixing ratio in different seasons at the two sites. In general, a high wind speed promoted a reduction in the $NH_3$ mixing ratio. Similar with other primary pollutants in Beijing, the $NH_3$ mixing ratios were high when winds originated from the south and low when winds originated from the north and northwest.

**Keywords:** $NH_3$; variations; simultaneous observation

## 1. Introduction

Ammonia ($NH_3$) is the most abundant alkaline trace gas in the atmosphere (Meng et al., 2017). An excessive $NH_3$ concentration directly harms the ecosystem; causes water eutrophication and soil acidification; and leads to forest soil erosion, biodiversity reduction, and carbon uptake variations (Pearson and Stewart, 1993; Reay et al., 2008; van Breemen et al., 1983). Thus, the $NH_3$ concentration influences climate change (Charlson et al., 1991; Erisman et al., 2007). $NH_3$ can react with acidic gases to form ammonium salts, which might significantly influence the mass concentration and composition of particulate matter (Wu et al., 2009). After the implementation of policies such as the *12th Five-Year Plan for the Key Regional Air Pollution Prevention and Control in Key Regions* (Ministry of Ecology and Environment of the People's Republic of China, 2012) and the *Air Pollution Prevention and Control Action Plan* (General Office of the State Council, PRC, 2013), China, especially for Beijing, has been effectively controlling the emission of primary pollutants, such as sulfur dioxide ($SO_2$) and nitrogen oxide ($NO_x$); however, the pollution caused by fine particles is still serious (Krotkov et al., 2016; UN Environment, 2019). Studies have indicated that when the $SO_2$ and $NO_x$ concentrations are reduced to a certain extent, reducing $NH_3$ emissions is the most economical and effective method to decrease the $PM_{2.5}$ concentration (Pinder et al., 2008). In China, the main anthropogenic sources of $NH_3$ are livestock and poultry feces (54%) and fertilizer volatilization (33%) (Huang et al., 2012). Moreover, the atmospheric $NH_3$ concentration in China has increased with the expansion of agricultural activities, control of $SO_2$ and $NO_x$, and increase in temperature (Warner et al., 2017). This increase in the $NH_3$ concentration might weaken the effectiveness of $SO_2$ and $NO_x$ emission control in reducing $PM_{2.5}$ pollution (Fu et al., 2017).

The North China Plain is a region with high $NH_3$ emission (Zhang et al., 2017), and Beijing has one of the highest $NH_3$ concentrations in the world (Chang et al., 2016b; Pan et al., 2018). Compared with studies on pollutants such as $SO_2$ and $NO_x$, considerably fewer studies have been conducted on the $NH_3$ concentration in Beijing. Chang et al. (2016a) collected gaseous $NH_3$ samples during the 2014 APEC summit (October 18 to November 29, 2014) in the Beijing urban area and concluded that the overall contributions of traffic, garbage, livestock, and fertilizers to the $NH_3$ concentration were 20.4%, 25.9%, 24.0%, and 29.7%, respectively. According the data from Huang et al (2012), the $NH_3$ emissions in Beijing were from livestock and poultry farming (34.55%), nitrogen-fixing plants (33.57%), fertilizer use (13.06%), household garbage treatment (8.29%), traffic emissions (5.20%), industrial emissions (0.14%), biomass combustion (0.42%), and agricultural soil (0.84%). Zhang (2016) measured the $NH_3$ concentrations in urban and rural areas of Beijing from January to July 2014 and found that $NH_3$ concentration in urban areas was approximately 65% higher than that in rural areas. Meng et al. (2011) reported that the highest $NH_3$ concentration in Beijing occurred in summer and the lowest one occurred in winter, and their results indicated traffic to be a significant source of $NH_3$ in urban areas. Zhang et al. (2018) reported the vertical variability of $NH_3$ in urban Beijing based on one-year passive samples in 2016/2017 and concluded that local sources such as traffic emissions were important contributors to urban $NH_3$. Meng *et al*. (2020) investigated the significant increase in winter $NH_3$ and its contribution to the increasing nitrate in $PM_{2.5}$ from 2009 to 2016, and they also concluded that vehicles exhaust was an important contributor to $NH_3$ in urban Beijing in winter.

Currently, $NH_3$ is not included in the routine environmental monitoring operation in China. Research data on $NH_3$ monitoring, particularly on the synchronous observation of the $NH_3$ concentrations with a high temporal resolution in urban and suburban areas, are relatively scarce. In this study, high-time-resolution observations of $NH_3$ were obtained simultaneously at an urban site and a suburban site in

Beijing. The variation characteristics and influencing factors of the $NH_3$ concentration were analyzed with meteorological data to provide a scientific basis for $NH_3$ pollution control in Beijing.

## 2. Materials and methods

### *2.1. Measurement sites*

From January 2018 to January 2019, continuous and simultaneous observations of the atmospheric $NH_3$ concentration were conducted in an urban area and a suburban in Beijing. The urban site was located on the roof of the Science and Technology Building of Minzu University of China (referred to as the urban site, 39.95°N, 116.32°E, altitude: 102 m) and the suburban site was in the Changping Meteorological Station (referred to as the suburban site, 40°13′N, 116°13′E, altitude: 77 m), respectively. The suburban site is in the NW direction relative to the urban site and the shortest distance between these two sites is approximately 32 km (Figure 1). More farm land and glass land are around the suburban site than the urban site.

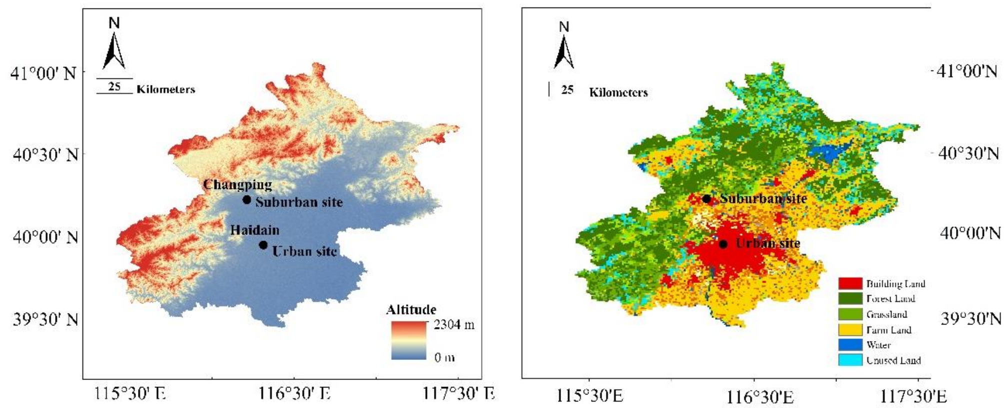


**Fig. 1.** Location of the observation sites, the topography, and land use of Beijing city.

### *2.2. Measurements and data acquisition*

$NH_3$ concentration measurements were performed by using two $NH_3$ analyzers (Ammonia Analyzer-Economical, Los Gatos Research Inc., USA), and the minimum detection limit was <0.2 ppb and the maximum drift of 0.2 ppb/24hrs. The analyzers were deployed in air-conditioning rooms. These analyzers use off-axis integrated cavity output spectroscopy (OA-ICOS) technology, which is a fourth-generation cavity-enhanced absorption technique, to measure the $NH_3$ and water vapor ($H_2O$) concentrations in the atmosphere. The incident laser beam of the OA-ICOS technology deviates from the optical axis, which differs from the traditional coaxial incidence mode. The axial incidence mode of the OA-ICOS technology can increase the optical path, stimulate additional high-order transverse modes, effectively suppress the noise of the cavity mode, reduce the cross interferences and errors due to contaminants existing in the cavity, and improve the detection sensitivity (Baer *et al*., 2002; Baer *et al*., 2012). The analyzer method is a quasi-absolute measurement, which theoretically does not require calibration. However, to ensure the comparability of the obtained data with other monitoring data, $NH_3$ standard gas (Beijing AP BAIF Gases Industry Co., Ltd.) was used for comparison measurement before the observation. The obtained concentration was revised with respect to a reference concentration.

Sample gases were drained by >0.4 L/min through Teflon lines (1/4'OD) from a manifold, which lengths were designed as short as possible (less than 2 m from the manifold). Particulate matters were filtered by Teflon membranes with a pore size less than 5 μm. Since $NH_3$ easily "sticks" to surfaces (like inside walls of tubes), heated sample lines were suggested by many measurements. However, according our test (Fig. S1) in the lab, when heating (70℃) was on, there did have a peak lasting several minutes (5–6 min) and then deceasing to the normal levels in ambient air, which means a new balancing process has been established in less than 10 min. This tells us that heating is not a solution for $NH_3$ sticking. Keeping the relatively stable balance between adsorption and desorption of $NH_3$ in the sampling system are the most important. When tested by different humidity air, only very sharply change of humidity obviously influenced and changed the balance, and a new balance needed tens of minutes to reestablished

(Fig. S2). In the routine weather conditions, humidity changed in a relatively smoothing way except in a quickly changing weather system, like rainy days. The minute-level data were converted into hourly averages in the data analysis process and the hourly resolution can smoothing the effect to some extent caused by variations in humidity and temperature during the sampling time.

The balancing idea was also used to carry out multiple calibrations on $NH_3$ analyzers (Fig. S3). A high mixing ratio (e.g. 400 ppb or higher) of $NH_3$ mixing gases were firstly produced by a dynamic diluter and measured by the $NH_3$ analyzer overnight. After the signals were keeping in stable level, other lower span values were switched in turn. At each span point, the measurement time was lasting at least 40 minutes or more. Then a linear regression function was obtained with $R^2$ higher than 0.999. Nowadays, $NH_3$ in compressed gas cylinder is also trustworthy, which result is concluded by the comparison with $NH_3$ permeation tube (Fig. S4).

Finally, 7645 and 8342 valid hourly mean observations were obtained for the urban (Haidian) and suburban (Changping) sites, respectively. In addition, the urban and suburban meteorological data (temperature, relative humidity, wind direction, and wind speed) during the sampling period were obtained from the Haidian Meteorological Observation Station and Changping Meteorological Station, respectively.

**3. Results and discussion**

*3.1. Overall variations in the $NH_3$ mixing ratios*

Fig. 2 displays the time-series variations in the $NH_3$ mixing ratios, temperatures, and relative humidity at the urban and suburban sites in Beijing. At the urban site, the mean ± 1σ, median, maximum, and minimum values of the hourly average $NH_3$ mixing ratio during the observation period were 21 ± 14, 17, 133 and 1.6 ppb, respectively. At the suburban site, the corresponding values were 22 ± 15, 18, 199, and 0.8 ppb, respectively. The annual average $NH_3$ mixing ratio and range of the $NH_3$ mixing ratio at the suburban site were marginally higher than those at the urban site. The variation characteristics of the weekly smoothing data indicated that the $NH_3$ variations and temperature/humidity fluctuations at the two sites were practically consistent, which suggested that both sites were under the influence of similar weather systems. The hourly mean $NH_3$ concentrations at the urban site were significantly correlated ($R$ = 0.849, $P < 0.01$) with those at the suburban site.

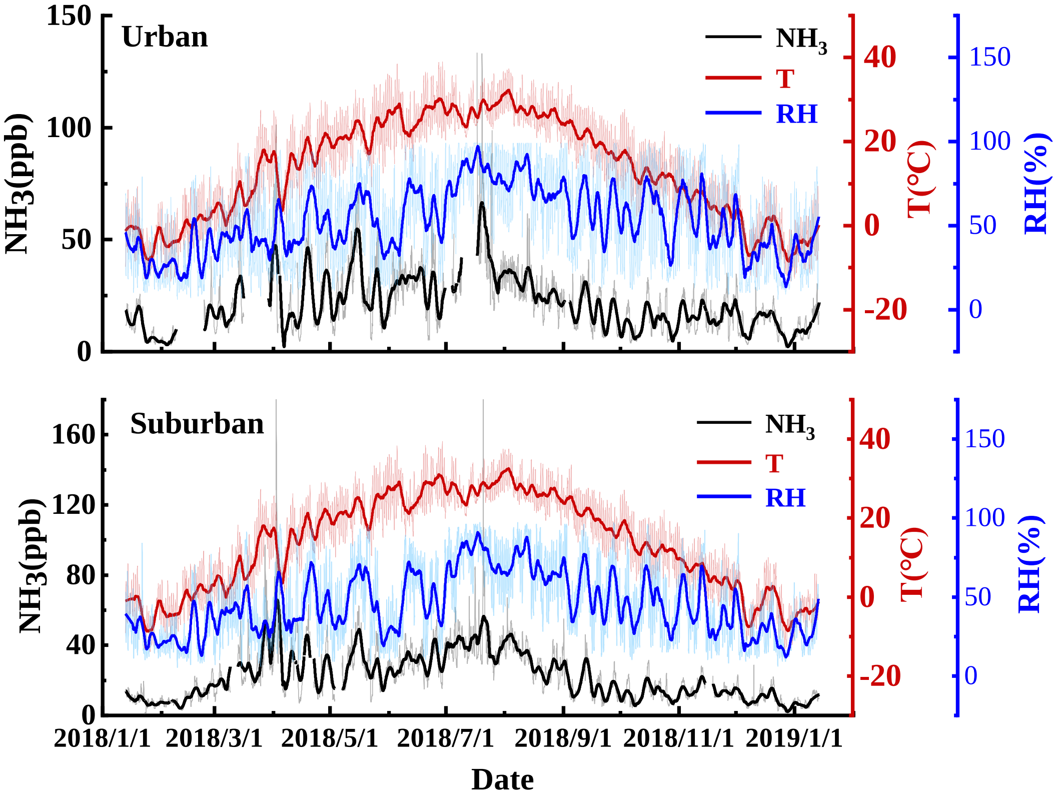


**Fig. 2.** Temporal variations in the hourly average $NH_3$ mixing ratios, temperatures ($T$) and relative humidity($RH$) at the urban and suburban stations in Beijing. Continuous thick lines were smoothed with 168 points (7 days) by using the Savitzky–Golay method.

Table 1 showed the comparison of the atmospheric $NH_3$ concentrations (ppb) in different areas. Meng et al. (2011) obtained an average $NH_3$ mixing ratio of 22.8 ± 16.3 ppb for the period 2008-2020 in Beijing urban area, which means there was no significant change in the annual average $NH_3$ mixing ratio from 2018 to 2019 compared with the change in the average $NH_3$ mixing ratio over the past decade.

Moreover, the $NH_3$ concentrations at the urban and suburban sites were higher than those in the background areas. The observed $NH_3$ concentrations in Beijing were higher than those in northwest China (Meng et al. 2010) and the Yangtze River Delta region (Chang et al. 2019). For example, the average annual $NH_3$ concentration in the urban area of Shanghai, a mega city in the south of China (31° N), was approximately 50% lower than that in Beijing. This result might be related to the fact that the North China Plain, in which Beijing is located, is one of the most intensive agricultural production regions in China. The differences in the soil properties of Beijing and Shanghai may be another reason because the loss of soil $NH_3$ can increase with an increase in the soil pH (Ju et al., 2009). Shanghai and its surrounding areas are dominated by acidic soil of paddy fields (Zhao et al., 2009), whereas Beijing is dominated by the alkaline soils of dry land (Wei et al., 2013).

**Table 1.** Comparison of the atmospheric $NH_3$ concentrations (ppb) in different areas.

| Period | Location | Methodology | Types | Concentration | Reference |
|---|---|---|---|---|---|
| 2018.01-2019.01 | Beijing, CN | Online monitor | Urban | 20.8±13.7 | This study |
| | | | Suburban | 21.9±14.9 | |
| 2008.02-2010.07 | Beijing, CN | Passive sampler | Urban | 22.8±16.3 | Meng et al., 2011 |
| 2007.01-2010.07 | | | Background | 10.2±10.8 | |
| 2014.5-2015.6 | Shanghai, CN | Passive sampler | Urban | 7.8 | Chang et al. 2019 |
| | | | Suburban | 6.8 | |
| 2006.04-2007.04 | Xi'an, CN | Passive sampler | Urban | 18.6 | Cao et al. 2009 |
| | | | Suburban | 20.3 | |
| 2017.12-2018.2 | Hebei, CN | Online monitor | Rural | 16.7±19.7 | He et al. 2020 |
| 2008 | Qinghai, CN | Passive sampler | Rural | 4.1±2.2 | Meng et al. 2010 |
| 2003.7-2011.9 | Toronto, CA | Passive sampler | Urban | 2.3-3.0 | Hu et al. 2014 |
| | | | Rural | 0.1-4 | |
| 2016.4-2017.10 | New York, US | Active and passive system | Urban | 2.2-3.2 | Zhou et al. 2019 |
| | | | Rural | 0.6-0.8 | |
| 2017.12 | Tokyo, JP | semi-continuous microflow analytical system | Urban | 4.1 | Osada et al. 2019 |
| 2013.1-2015.12 | Delhi, IN | Automatic analyzer | Urban | 53.4±14.9 | Saraswati et al., 2019 |
| 2012.10-2013.9 | Jaunpur, IN | Glass flask sampling | Suburban | 51.6±22.8 | Singh and Kulshrestha, 2014 |
| 2008.1-2009.2 | Bamako, MLI | Passive sampler | Urban | 46.7 | Adon et al., 2016 |

| | | | | | |
|---|---|---|---|---|---|
| 2006.3-2017.4 | Edmonton, CA | Online monitor | Urban | 2.4±0.6 | Yao et al., 2016 |
| 2010.9-2011.8 | Seoul, KR | Online monitor | Urban | 10.9±4.25 | Phan et al., 2013 |
| 2004.3-2004.7 | Munster, DE | Wet denuder | Urban | 5.2 | Vogt et al., 2005 |

The $NH_3$ mixing ratios in the United States (Edgerton et al., 2007; Nowak et al., 2006; Zhou et al. 2019), Great Britain (Burkhardt et al., 1998), Canada (Hu et al., 2014), and Japan (Osada et al., 2019) were 0.23–13, 1.6–2.3, 0.1–4, and 4.1 ppb, respectively. These $NH_3$ mixing ratios are considerably lower than that in Beijing. However, Delhi, India (Saraswati et al., 2019), exhibited a higher $NH_3$ mixing ratio (53.4±14.9 ppb) than Beijing did. This result might be attributed to the well-developed livestock breeding activities in Delhi. The comparisons indicate that in the past decade, $NH_3$ concentration in Beijing has not changed considerably, but that it is higher than in large cities in other developed countries.

*3.2. Seasonal variations*

Fig. 2 displays the monthly statistical results for the $NH_3$ mixing ratios at the urban and suburban sites in Beijing. According to the seasonal division standard of China Meteorological Administration, in China, March to May is spring, June to August is summer, September to November is autumn, and December to February is winter. As presented in Fig. 2, the seasonal variations in the $NH_3$ mixing ratios were very similar at the urban and suburban sites. The $NH_3$ mixing ratios showed high values in the spring and summer and low values in the autumn and winter. The daily mean concentrations fluctuated considerably in the spring, and the highest variations occurred in April. The highest mean $NH_3$ concentrations occurred in July. The highest mean $NH_3$ concentrations at the urban and suburban sites were 42± 17 ppb and 42 ± 8.2 ppb, respectively. The $NH_3$ concentrations fluctuated considerably in July. On average, the $NH_3$ mixing ratios at the urban and suburban sites can be arranged according to season as follows: summer > spring > autumn > winter. The main grain crops in Beijing are corn and wheat.

Corn is categorized as spring corn and summer corn, which are sown in April and June, respectively. A large amount of base fertilizer is applied when planting corn, and the topdressing is applied after 2 months. Wheat is sown from September to October, and the topdressing is applied in the following spring. The volatilization of nitrogen fertilizers can cause an increase in the $NH_3$ mixing ratios and fluctuations in fertilization seasons (Zhang et al., 2016). In addition, the $NH_3$ mixing ratios are relatively high in the summer season due to the relatively high temperature in this season. An increase in the temperature can increase the biological activity and thus enhance the $NH_3$ emission. A high temperature is also conducive for the volatilization of the urea and diammonium phosphate applied to crops. Moreover, the equilibrium among ammonium nitrate particles, gaseous $NH_3$, and nitric acid is transferred to the gas phase at high temperature, which increases $NH_3$ concentration (Behera et al., 2013). Sewage treatment, household garbage, golf courses, and human excreta are crucial $NH_3$ sources that are easily neglected (Pu et al., 2020). The relatively low $NH_3$ concentrations in the autumn and winter might be caused by the decrease in $NH_3$ emission in the soil and vegetation, the decrease in the $NH_4NO_3$ decomposition capacity at low temperatures, and the reduced human activities caused by a large floating population returning to their native locations outside Beijing during the Spring Festival (Liao et al., 2014). In the spring and summer, the $NH_3$ mixing ratios at the suburban site were higher than those at the urban site, which might be related to the higher agricultural activity around the suburban site. In the autumn and winter, the $NH_3$ mixing ratios at the urban site were marginally higher than those at the suburban site. This result was obtained possibly because in the autumn and winter seasons, the influence of agricultural activities on the $NH_3$ concentration weakened, whereas the influences of other sources (such as traffic sources) on the $NH_3$ concentration were enhanced. According to Wang et al. (2019), the traffic $NH_3$ emission per unit area in Haidian was three times higher than that in Changping. This difference in traffic source emissions might have resulted in higher $NH_3$ concentrations at the urban site than at the suburban site in the autumn and winter.

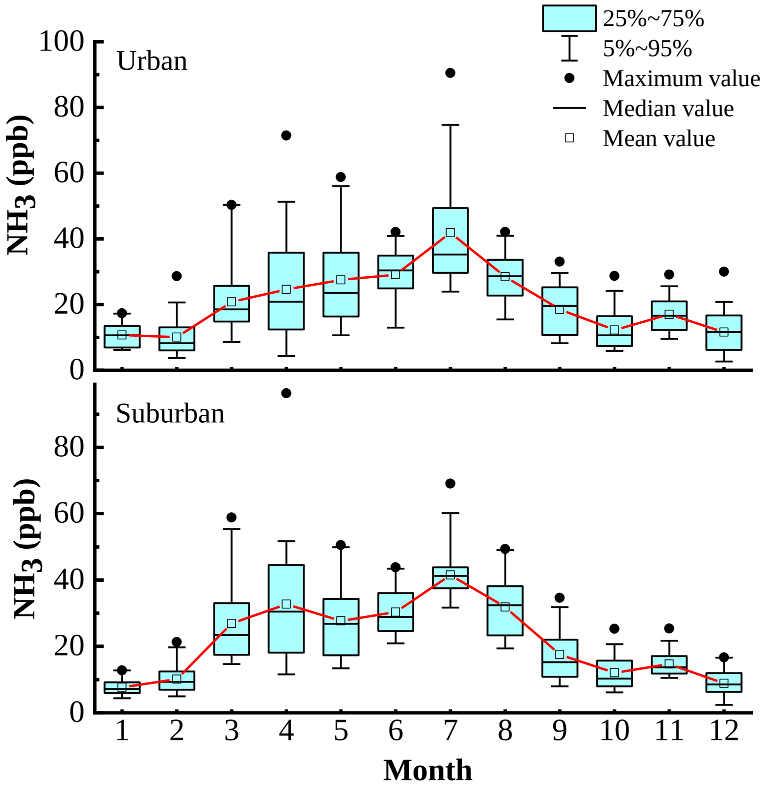


**Fig. 3.** Monthly statistical variation in the $NH_3$ mixing ratios at the urban and suburban sites in Beijing.

**Table 2.** $NH_3$ mixing ratios (ppb) measured at the urban and suburban sites in Beijing.

| Site | Time period | Mean | Standard deviation | Minimum | Median | Maximum |
|---|---|---|---|---|---|---|
| Urban | Annual | 21 | 14 | 1.6 | 17 | 133 |
| | Spring | 25 | 16 | 1.9 | 21 | 101 |
| | Summer | 32 | 12 | 5.0 | 30 | 133 |
| | Autumn | 16 | 7.5 | 3.8 | 15 | 41 |
| | Winter | 11 | 6.7 | 1.6 | 9.9 | 42 |
| Suburban | Annual | 22 | 15 | 0.8 | 18 | 198 |
| | Spring | 29 | 16 | 6.8 | 26 | 180 |
| | Summer | 35 | 12 | 12.1 | 33 | 199 |
| | Autumn | 15 | 6.8 | 4.1 | 13 | 55 |

| | | | | | |
|---|---|---|---|---|---|
| Winter | 9.2 | 4.5 | 0.8 | 8.4 | 29 |

*3.3. Diurnal variations*

Figure 4 displays the average diurnal variations in the $NH_3$ and $H_2O$ mixing ratios in different seasons at the urban and suburban sites in Beijing. $NH_3$ exhibited different diurnal behaviors in different seasons.

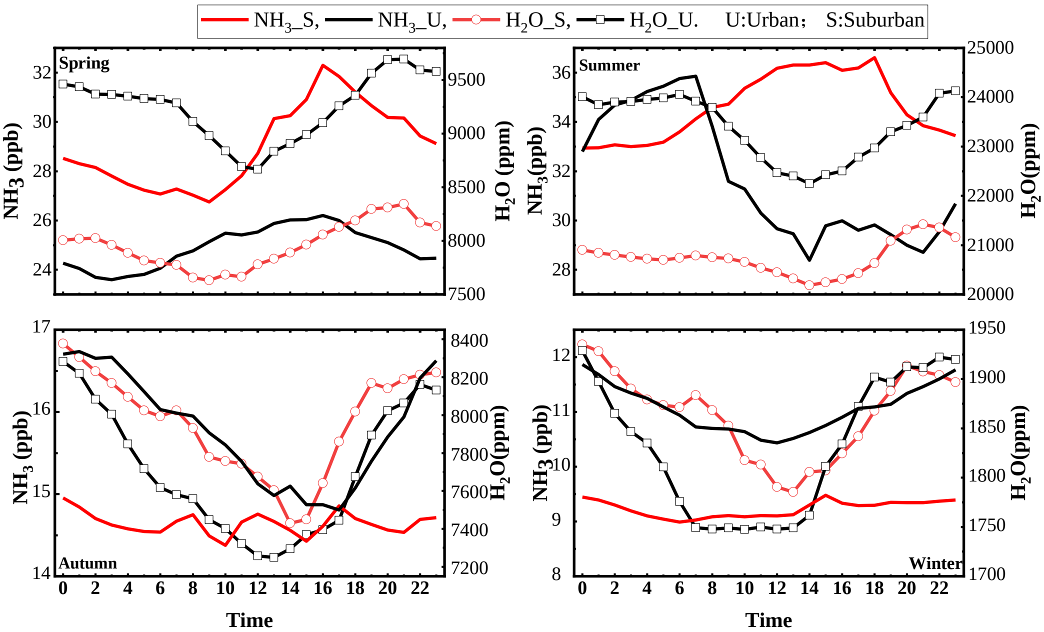


**Fig. 4.** Average diurnal variations in the $NH_3$ and $H_2O$ mixing ratios in different seasons at the urban and suburban sites in Beijing.

In the spring, the average diurnal variations in the $NH_3$ mixing ratio were similar at the urban and suburban sites. The diurnal variations exhibited a single-peak pattern with high values in the daytime and low values at night. The $NH_3$ mixing ratio began to increase in the morning, reached its maximum value at 16:00, and then decreased gradually. The lowest mixing ratios at the urban and suburban sites occurred at 03:00 and 09:00, respectively. The $NH_3$ mixing ratio began to increase earlier at the urban site than at the suburban site. This result was obtained possibly due to the increased $NH_3$ emission at the urban site due to traffic in the morning rush hours. On average, the mixing ratio of $NH_3$ was considerably higher at the suburban site than that at the urban site, with an average difference of 4.1 ppb and a maximum difference of 6.1 ppb in the $NH_3$ mixing ratios of the sites. The average fluctuation in the $NH_3$ mixing ratio at the suburban site was 5.3 ppb, which was higher than that (2.6 ppb) at the urban site. At the urban site, the average diurnal variations in the $NH_3$ and $H_2O$ mixing ratios exhibited opposite trends. The $H_2O$ mixing ratio had high values in the night and low values in the day. At the suburban site, the variation characteristics of $NH_3$ and $H_2O$ were very similar; however, the peak $NH_3$ concentration occurred 5 hours earlier than the peak $H_2O$ concentration. In the spring, in contrast to the $NH_3$ mixing ratio, the $H_2O$ mixing ratio at the urban site was 1279 ppm higher than that at the suburban site.

The diurnal variations in the $NH_3$ mixing ratio at the suburban site in the summer were similar with those in the spring. This phenomenon was also observed in the rural areas of Shanghai by Chang et al. (2019). The diurnal variations were considerably affected by the temperature and the contribution from volatile $NH_3$ sources. However, at the urban site, the diurnal variations in the $NH_3$ mixing ratio were different. In the summer, the $NH_3$ mixing ratio increased gradually from 21:00, decreased after reaching its peak value at 7:00, and then reached its lowest value at 14:00. The diurnal variability pattern (with a peak value in the morning) has been observed in other areas, such as rural (Ellis et al., 2011), urban (Gong et al., 2011), and steppe areas located far away from human activity (Wentworth et al., 2016). Kuang et al. (2020) believed that the diurnal variability pattern was caused by the evaporation of dew in the morning, which results in the release of $NH_3$ that was originally stored in the droplets. A lag was observed between the changes in the $NH_3$ with $H_2O$ concentrations in the early morning, which supported the hypothesis of Kuang et al (2020). In addition, the increase in the $NH_3$ concentration in the morning might have been caused by the breakup of the boundary layer formed at night. The downward mixing of air with a high $NH_3$ concentration in the residual layer led to an increase in the $NH_3$ concentration on the ground in the morning (Bash et al., 2010). The $NH_3$ and $H_2O$ concentrations at the urban and suburban sites exhibited opposite diurnal variations patterns in the spring. In the summer, the $NH_3$ concentrations at the suburban site were significantly higher than those at the urban site during the daytime and first half of the night. However, the $NH_3$ concentrations at the urban site were significantly higher than those at the suburban site during the second half of the night. The average fluctuation in the $NH_3$ concentration was 7.5 and 37 ppb at the urban and suburban site, respectively. Similar with the situation in the spring, the $H_2O$ concentrations at the urban site were significantly higher than those at the suburban site in the summer.

In the autumn, the $NH_3$ concentration at the urban site had low values during the day and high values during the night. The peak $NH_3$ concentration occurred at midnight, and the lowest $NH_3$ concentration occurred at 17:00. There was essentially no diurnal variation in the $NH_3$ concentration at the suburban site, but obvious at the urban site with a fluctuation of 2.0 ppb. The concentration of $NH_3$ at the urban site was 1.2 ppb higher than that at the suburban site. The $H_2O$ concentration was marginally lower (250 ppm) at the urban site than at the suburban site. The correlation between the diurnal variations in the $NH_3$ and $H_2O$ concentrations was strong; however, the lowest value of $NH_3$ occurred later than the lowest value of $H_2O$ at the urban site. The correlation between the diurnal variations in the $NH_3$ and $H_2O$ concentrations was poor at the suburban site.

In the winter, the $NH_3$ mixing ratios at the urban and suburban sites exhibited similar diurnal variation patterns. The mixing ratios exhibited high values in the night and low values in the day. However, the $NH_3$ mixing ratio at the urban site was higher than that at the suburban site. This result was related to the decrease in the boundary layer height and temperature as well as the slow conversion and easy accumulation of pollutants in the night. In the daytime, increases in the temperature and boundary layer height enhanced the diffusion of pollutants, and the $NH_3$ mixing ratio decreased. The $H_2O$ mixing ratio at the suburban site was close to that at the urban site, but higher in the morning. In the winter, the average diurnal variation in the $NH_3$ concentration was well correlated with that in the $H_2O$ concentration at the urban site ($R$ = 0.89). The correlation was close to that ($R$ = 0.93) obtained by Teng et al. (2017) between the $NH_3$ and $H_2O$ concentrations in the winter. However, at the suburban site, the mean diurnal variation in the $NH_3$ mixing ratios had a poor correlation with that in the $H_2O$ mixing ratios.

The results indicated that although the two sites were under the influence of similar weather systems, the diurnal variations in the $NH_3$ mixing ratios at the two sites were different in different seasons. This finding suggested that different $NH_3$ sources and possibly sinks had different contributions to the $NH_3$ concentrations at the urban and suburban sites. Additional studies should be conducted on the behaviors of $NH_3$.

*3.4. Effect of meteorological factors on the $NH_3$ levels*

Table 3 presents the correlations between the daily mean $NH_3$ mixing ratios and the diurnal mean values of the temperature, relative humidity, and wind speed at the two sites. Annually, the correlations were highly significant as the $NH_3$ mixing ratios at both sites were significantly and positively correlated with the temperature and relative humidity and negatively correlated with the wind speed. However, in the summer and autumn, no significant correlations were noted between the $NH_3$ and temperature at the two sites. The relative humidity had the stronger influence on the $NH_3$ concentration at the two sites than temperature, which phenomenon also can be found in Fig 2. The fluctuations between $NH_3$ and relative humidity were much more consistent.

Table 3. Correlations between the daily mean values of $NH_3$ and meteorological elements (Spearman's rank correlation coefficient)

| Site | Time Period | Temperature | Relative humidity | Wind speed |
|---|---|---|---|---|
| | Annual | 0.680** | 0.706** | -0.370** |
| | Spring | 0.450** | 0.645** | -0.540** |
| Urban | Summer | 0.043 | 0.488** | -0.106** |
| | Autumn | 0.101 | 0.759** | -0.413** |
| | Winter | 0.596** | 0.690** | -0.449** |
| | Annual | 0.745** | 0.730** | -0.325** |
| | Spring | 0.256* | 0.518** | -0.391** |
| Suburban | Summer | 0.126 | 0.576** | -0.061** |
| | Autumn | 0.135 | 0.792** | -0.618** |
| | Winter | 0.676** | 0.663** | -0.545** |

*: at the 0.05 significant level; **: at the 0.01 significant level.

Figs. 5 display the seasonal mean diurnal variations in the $NH_3$ mixing ratio, temperature, and relative humidity with their correlation coefficients (also see in Fig. S5) in different seasons at the urban and suburban sites. At urban site, the diurnal variations in the $NH_3$ mixing ratio at the urban site were positively (negatively) correlated with the temperature (relative humidity) in spring, while in contrast, the diurnal variation of $NH_3$ mixing ratio were negatively (positively) correlated with temperature (relative humidity) in summer and autumn, and less correlated in winter. At suburban site, the diurnal variations in the $NH_3$ mixing ratio were positively (negatively) correlated with the temperature (relative humidity) in the spring and summer, but less correlated in the fall and winter. Similar behaviors were found in spring, but different in other seasons. In general, the annual diurnal behaviors of $NH_3$ with temperature and relative humidity were different at the urban and suburban sites (see Fig. S6). Figure 6 displays the contour maps of the $NH_3$ mixing ratio, temperature, and relative humidity in different seasons at the urban and suburban sites. As displayed in Fig. 6 and Fig. S7, the $NH_3$ mixing ratios at both sites increased with the relative humidity at the same temperature and increased with the temperature at the same relative humidity. In winter, when the temperature was low (< 0 °C), the $NH_3$ mixing ratios at both sites often had low values except in high humidity (>60%). An increase in the temperature increased the $NH_3$ mixing ratios; however, the $NH_3$ concentration at the suburban site was more significantly affected by the temperature than that at the urban site (Table 3), indicating that volatile $NH_3$ sources might have a higher contribution to the $NH_3$ concentration at the suburban site than at the urban site. A higher amount of $NH_3$ removal through chemical transformation was expected during the day at the urban site than at the suburban site because the urban site had a higher relative humidity and higher amounts of primary particulate matter, $NO_x$, and $SO_2$ acid gas emissions than the suburban site did. In 2018, the concentrations of $PM_{2.5}$, $SO_2$ and $NO_2$ were 50μg/m$^3$, 5μg/m$^3$, 43μg/m$^3$ in Haidian, and 46μg/m$^3$, 6μg/m$^3$, 35μg/m$^3$ in Changping, respectively, which were reported by Beijing Ecology and Environment Statement, 2018.

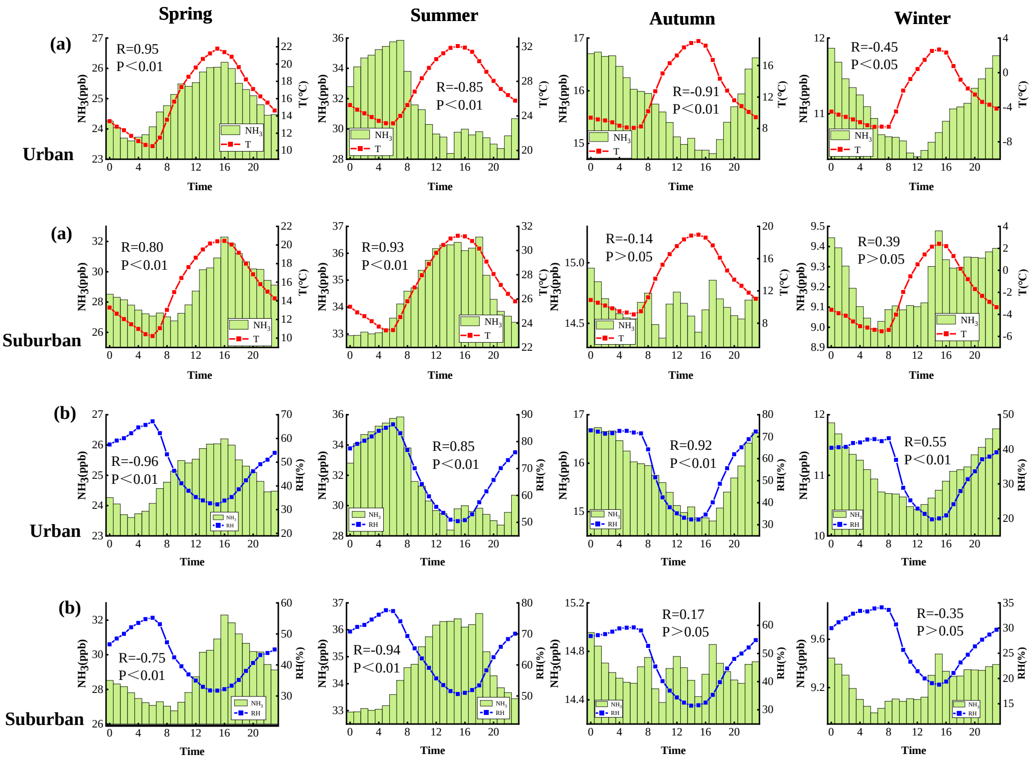


**Fig. 5.** Diurnal variations in and correlation coefficients between the $NH_3$ mixing ratios and temperature (a), relative humidity (b) in different seasons at the urban and suburban sites in Beijing.

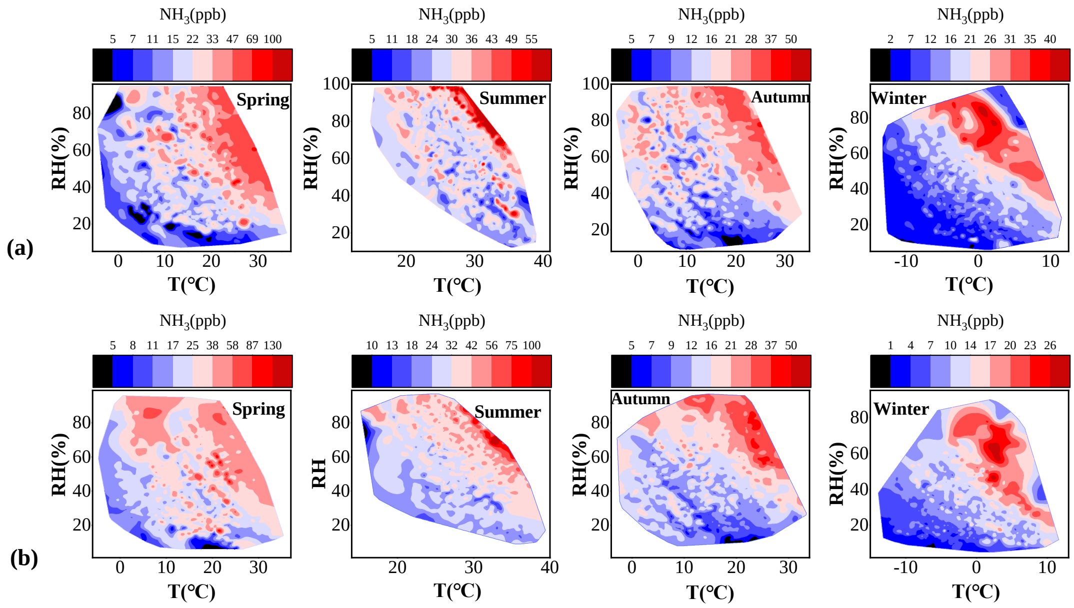


**Fig. 6.** Contour maps of the $NH_3$ mixing ratio, temperature, and relative humidity in different seasons at the urban and suburban sites in Beijing (a: Urban, b: Suburban).

To explore the influence of wind on the $NH_3$ mixing ratios, rose charts were drawn for the hourly mean concentration of $NH_3$, wind direction frequency, and wind speed during the observation period (Fig. 7). The large-scale wind circulation in the North China Plain is often influenced by the mountain-plain topography; therefore, the dominant winds in this area originate from the south (often in the day) and north (often at night). As displayed in Fig. 6, some differences existed in the distributions of the surface wind between the urban and suburban sites. The dominant surface winds originated from the northeast and southwest at the urban site and from the northwest and east at the suburban site. At the urban site, the $NH_3$ mixing ratios were relatively high when the winds originated from the southern sectors and relatively low when the winds originated from the northwest sectors. Therefore, under the action of the southwest wind, a polluted air mass from the south of Beijing can be easily transported to the urban site. Meng et al. (2017) examined the effect of long-range air transport on the urban $NH_3$ levels in Beijing during the summer through trajectory analysis. The authors concluded that the air mass from the southeast has a cumulative effect on the $NH_3$ concentration. Although the dominant wind direction at the suburban site was different from that at the urban site, the $NH_3$ mixing ratios were relatively high in the south sectors for both sites. Thus, winds from the southeast, south, and southwest had a cumulative effect on the $NH_3$ mixing ratios at both the urban and suburban sites. The $NH_3$ mixing ratios were relatively low when the wind originated from the northwest sector at urban site and from the west sector at the suburban site, in which the wind speed was strong, which indicated that the northwest/west wind could promote $NH_3$ dilution and diffusion.

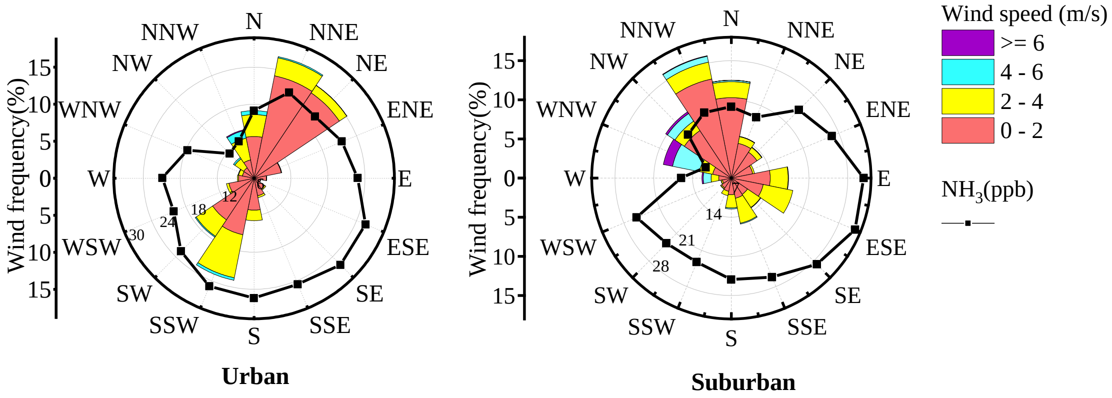


**Fig. 7.** Rose maps of the $NH_3$ mixing ratios, wind frequency, and wind speed in different wind direction sectors.

Heavy rainfall occurred on a few days in Beijing in 2018. Heavy precipitation occurred for a long duration on August 18, 2018 (Fig. 8). Before the rainfall, the $NH_3$ concentration at the urban site was higher than the average level in August. After the rainfall occurred, the $NH_3$ concentration decreased rapidly, and it was significantly lower than the mean value in August. However, the diurnal variation of $NH_3$ on the rain day did not differ considerably from the average diurnal variation in August. On August 18, 2018, the $NH_3$ mixing ratio at the suburban site remained at a low level during the rainfall period and was considerably lower than the mean $NH_3$ concentration in August. However, the $NH_3$ mixing ratio increased rapidly after the precipitation and reached the mean level at 17:00. The rainfall might have an obvious clearing effect on $NH_3$ but needed more cases to support.

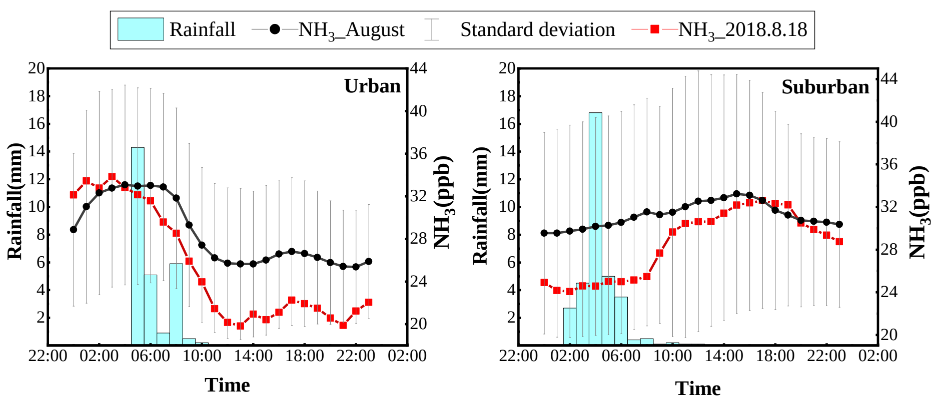


**Fig. 8.** Diurnal variations in the rainfall and $NH_3$ concentration on August 18, 2018.

## 4. Conclusion

In this study, the atmospheric $NH_3$ concentrations at an urban site and a suburban site in Beijing were continuously and simultaneously observed from January 2018 to January 2019. The mean $NH_3$ mixing ratios were 21 ± 14 and 22 ± 15 ppb at the urban and suburban sites, respectively. The annual average $NH_3$ mixing ratio at the suburban site was higher than that at the urban site. Moreover, the variation range of the $NH_3$ mixing ratio was larger at the suburban site than at the urban site. In the summer and spring, the $NH_3$ mixing ratio at the suburban site was higher than that at the urban site. In the autumn and winter, the $NH_3$ mixing ratio at the suburban site was lower than that at the urban site. The highest $NH_3$ mixing ratios at the urban and suburban sites were observed in July. The lowest $NH_3$ mixing ratio at the urban site occurred in February, and the lowest $NH_3$ mixing ratio at the suburban site occurred in January. In the past decade, the concentration of $NH_3$ in Beijing did not change considerably, and the $NH_3$ levels in Beijing were higher than those in other large cities.

The hourly mean $NH_3$ mixing ratios at the urban site were highly correlated ($R = 0.849$, $P < 0.01$) with those at the suburban site. However, the mean diurnal variations in the $NH_3$ mixing ratios at the urban and suburban sites were different. At the urban site, low $NH_3$ mixing ratios were observed in the day and high $NH_3$ mixing ratios were observed in the night. The opposite trend was observed at the suburban site. Although both sites were under the influence of similar weather systems, the seasonal diurnal variations in the $NH_3$ mixing ratio were different at the urban and suburban sites. This result indicated that $NH_3$ sources had different contributions to the $NH_3$ levels at the urban and suburban sites.

The influence of meteorological factors on the $NH_3$ mixing ratio was complex. At the same temperature, the $NH_3$ mixing ratios increased with the relative humidity at the urban and suburban sites.

At the same relative humidity, the $NH_3$ mixing ratios increased with the temperature at both sites. The relative humidity had the strongest influence on the $NH_3$ mixing ratio in different seasons at the two sites. No strong correlation was observed between the $NH_3$ concentration and the temperature in the summer and autumn at the two sites. A high wind speed promoted a decrease in the $NH_3$ concentration. The $NH_3$ mixing ratios were higher when the winds originated from the south than when the winds originated from the north and northwest. Rainfall had a certain scavenging effect on $NH_3$; however, it had little effect on the diurnal variations in the $NH_3$ concentration.

***Data availability*.** The data of stationary measurements are available upon request to the contact author Weili Lin (linwl@muc.edu.cn).

***Author contributions*.** ZL and WL developed the idea for this paper, formulated the research goals, and carried out the measurement at urban site. WP and ZM carried out the $NH_3$ field observations at the suburban site.

**Competing interests.** The authors declare that they have no conflict of interest.

**Acknowledgments.** This study was funded by the National Natural Science Foundation of China (Grant No. 91744206) and the Beijing Municipal Science and Technology (Z181100005418016).

**Reference**

Adon, M., Yoboué, V., Galy-Lacaux, C., Liousse, C., Diop, B., Doumbia, E. H. T., Gardrat, E., Ndiaye, S. A. and Jarnot, C.: Measurements of $NO_2$, $SO_2$, $NH_3$, $HNO_3$ and $O_3$ in West African urban environments, Atmospheric Environment, 135, 31–40, https://doi.org/10.1016/j.atmosenv.2016.03.050, 2016.

Baer, D. S., Paul, J. B., Gupta, M. and O'Keefe, A.: Sensitive absorption measurements in the near-infrared region using off-axis integrated-cavity-output spectroscopy, Applied Physics B: Lasers and Optics, 75(2–3), 261–265, doi:10.1007/s00340-002-0971-z, 2002.

Baer, D., Gupta, M., Leen, J. B., and Berman, E.: Environmental and atmospheric monitoring using off-axis integrated cavity output spectroscopy (OA-ICOS). American laboratory, 44(10), 20–23, 2012.

Bash, J. O., Walker, J. T., Katul, G. G., Iones, M. R., Nemitz, E. and Robarge, W. P.: Estimation of in-canony ammonia sources and sinks in a fertilized zea mays field, Environmental Science and Technology, 44(5), 1683-1689, doi:10.1021/es9037269, 2010.

Behera, S. N., Sharma, M., Aneja, V. P. and Balasubramanian, R.: Ammonia in the atmosphere: A review on emission sources, atmospheric chemistry and deposition on terrestrial bodies, Environmental Science and Pollution Research, 20(11), 8092–8131, doi:10.1007/s11356-013-2051-9, 2013.

Breemen, N. V., Mulder, J. and Driscoll, C. T.: Acidification and alkalinization of soils, Plant and Soil, 75(3), 283–308, doi:10.1007/BF02369968, 1983.

Burkhardt, J., Sutton, M. A., Milford, C., Storeton-West, R. L. and Fowler, D.: Ammonia concentrations at a site in southern Scotland from 2 yr of continuous measurements, in

Atmospheric Environment, 32(3), 325–331, https://doi.org/10.1016/S1352-2310(97)00198-2.

Chang, Y., Liu, X., Deng, C., Dore, A. J. and Zhuang, G.: Source apportionment of atmospheric ammonia before, during, and after the 2014 APEC summit in Beijing using stable nitrogen isotope signatures, Atmospheric Chemistry and Physics, 16(18), doi:10.5194/acp-16-11635-2016, 2016a.

Chang, Y., Zou, Z., Deng, C., Huang, K., Collett, J. L., Lin, J. and Zhuang, G.: The importance of vehicle emissions as a source of atmospheric ammonia in the megacity of Shanghai, Atmospheric Chemistry and Physics, 16(5), 3577-3594, doi:10.5194/acp-16-3577-2016, 2016b.

Chang, Y., Zou, Z., Zhang, Y., Deng, C., Hu, J., Shi, Z., Dore, A. J. and Collett, J. L.: Assessing Contributions of Agricultural and Nonagricultural Emissions to Atmospheric Ammonia in a Chinese Megacity, Environmental Science and Technology, 53(4), 1822–1833, doi:10.1021/acs.est.8b05984, 2019.

Charlson, R.J., LANGNER, J., Rodhe, H., Leovy, C.B., Warren, S.G.: Perturbation of the northern hemisphere radiative balance by backscattering from anthropogenic sulfate aerosols, Tellus B: Chemical and Physical Meteorology, 43(4),12, doi:10.1034/j.1600-0889.1991.t01-1-00013.x, 1991.

Edgerton, E. S., Saylor, R. D., Hartsell, B. E., Jansen, J. J. and Alan Hansen, D.: Ammonia and ammonium measurements from the southeastern United States, Atmospheric Environment, 41(16), 3339-3351, doi:10.1016/j.atmosenv.2006.12.034, 2007.

Ellis, R. A., Murphy, J. G., Markovic, M. Z., Vandenboer, T. C., Makar, P. A., Brook, J. and Mihele, C.: The influence of gas-particle partitioning and surface-atmosphere exchange on ammonia during BAQS-Met, Atmospheric Chemistry and Physics, 11(1), 133-145, doi:10.5194/acp-11-133-2011, 2011.

Erisman, J. W., Bleeker, A., Galloway, J. and Sutton, M. S.: Reduced nitrogen in ecology and the environment, Environmental Pollution, 150(1), 140-149, doi:10.1016/j.envpol.2007.06.033, 2007.

Fu, X., Wang, S., Xing, J., Zhang, X., Wang, T. and Hao, J.: Increasing Ammonia Concentrations Reduce the Effectiveness of Particle Pollution Control Achieved via $SO_2$ and $NO_X$ Emissions Reduction in East China, Environmental Science and Technology Letters, 4(6), 221–227, doi:10.1021/acs.estlett.7b00143, 2017.

Gong, L., Lewicki, R., Griffin, R. J., Flynn, J. H., Lefer, B. L. and Tittel, F. K.: Atmospheric ammonia measurements in Houston, TX using an external-cavity quantum cascade laser-based sensor, Atmospheric Chemistry and Physics, 11(18), 9721–9733, doi:10.5194/acp-11-9721-2011, 2011.

Hu, Q., Zhang, L., Evans, G. J. and Yao, X.: Variability of atmospheric ammonia related to potential emission sources in downtown Toronto, Canada, Atmospheric Environment, 99, doi:10.1016/j.atmosenv.2014.10.006, 2014.

Huang, X., Song, Y., Li, M., Li, J., Huo, Q., Cai, X., Zhu, T., Hu, M. and Zhang, H.: A high-resolution ammonia emission inventory in China, Global Biogeochemical Cycles, 26(1), doi:10.1029/2011GB004161, 2012.

Ju, X. T., Xing, G. X., Chen, X. P., Zhang, S. L., Zhang, L. J., Liu, X. J., Cui, Z. L., Yin, B., Christie, P., Zhu, Z. L. and Zhang, F. S.: Reducing environmental risk by improving N management in intensive Chinese agricultural systems, Proceedings of the National Academy of Sciences of the United States of America, 106(9), 3041-3046, doi:10.1073/pnas.0813417106, 2009.

Krotkov, N.A., McLinden, C.A., Li, C., Lamsal, L.N., Celarier, E.A., Marchenko, S. v., Swartz, W.H., Bucsela, E.J., Joiner, J., Duncan, B.N., Boersma, K.F., Veefkind, J.P., Levelt, P.F., Fioletov, V.E., Dickerson, R.R., He, H., Lu, Z., Streets, D.G.: Aura OMI observations of regional $SO_2$ and $NO_2$

pollution changes from 2005 to 2015. Atmospheric Chemistry and Physics 16(7), 4605–4629, doi:10.5194/acp-16-4605-2016, 2016.

Kuang, Y., Xu, W., Lin, W., Meng, Z., Zhao, H., Ren, S., Zhang, G., Liang, L. and Xu, X.: Explosive morning growth phenomena of NH3 on the North China Plain: Causes and potential impacts on aerosol formation, Environmental Pollution, 257, 113621, doi:10.1016/j.envpol.2019.113621, 2020.

Liao, X., Zhang, X., Wang, Y., Liu, W., Du, J. and Zhao, L.: Comparative Analysis on Meteorological Condition for Persistent Haze Cases in Summer and Winter in Beijing, Environmental Science, 35(06), 2031–2044, doi:10.13227/j.hjkx.2014.06.001, 2014.

Meng, Z. Y., Lin, W. L., Jiang, X. M., Yan, P., Wang, Y., Zhang, Y. M., Jia, X. F. and Yu, X. L.: Characteristics of atmospheric ammonia over Beijing, China, Atmospheric Chemistry and Physics, 11(12), 6139–6151, doi:10.5194/acp-11-6139-2011, 2011.

Meng, Z. Y., Xu, X. bin, Wang, T., Zhang, X. Y., Yu, X. L., Wang, S. F., Lin, W. L., Chen, Y. Z., Jiang, Y. A. and An, X. Q.: Ambient sulfur dioxide, nitrogen dioxide, and ammonia at ten background and rural sites in China during 2007–2008, Atmospheric Environment, 44(21–22), 2625-2631, doi:10.1016/j.atmosenv.2010.04.008, 2010.

Meng, Z., Lin, W., Zhang, R., Han, Z. and Jia, X.: Summertime ambient ammonia and its effects on ammonium aerosol in urban Beijing, China, Science of the Total Environment, 579, 1521–1530, doi:10.1016/j.scitotenv.2016.11.159, 2017.

Meng, Z., Wu, L., Xu, X., Xu, W., Zhang, R., Jia, X., Liang, L., Miao, Y., Cheng, H., Xie, Y., He, J. and Zhong, J.: Changes in ammonia and its effects on $PM_{2.5}$ chemical property in three winter seasons in Beijing, China, Science of The Total Environment, 749, 142208, doi:10.1016/j.scitotenv.2020.142208, 2020.

Nowak, J. B., Huey, L. G., Russell, A. G., Tian, D., Neuman, J. A., Orsini, D., Sjostedt, S. J., Sullivan, A. P., Tanner, D. J., Weber, R. J., Nenes, A., Edgerton, E. and Fehsenfeld, F. C.: Analysis of urban gas phase ammonia measurements from the 2002 Atlanta Aerosol Nucleation and Real-Time Characterization Experiment (ANARChE), Journal of Geophysical Research Atmospheres, 111(17), doi:10.1029/2006JD007113, 2006.

Osada, K., Saito, S., Tsurumaru, H. and Hoshi, J.: Vehicular exhaust contributions to high $NH_3$ and $PM_{2.5}$ concentrations during winter in Tokyo, Japan, Atmospheric Environment, 206, 218–224, doi:10.1016/j.atmosenv.2019.03.008, 2019.

Pan, Y., Tian, S., Zhao, Y., Zhang, L., Zhu, X., Gao, J., Huang, W., Zhou, Y., Song, Y., Zhang, Q. and Wang, Y.: Identifying Ammonia Hotspots in China Using a National Observation Network, Environmental Science and Technology, 52(7), 3926–3934, doi:10.1021/acs.est.7b05235, 2018.

Pearson, J. and Stewart, G.R.: The deposition of atmospheric ammonia and its effects on plants, New Phytologist, 125(2), 283–305, doi:10.1111/j.1469-8137.1993.tb03882.x, 1993.

Phan, N.-T., Kim, K.-H., Shon, Z.-H., Jeon, E.-C., Jung, K. and Kim, N.-J.: Analysis of ammonia variation in the urban atmosphere, Atmospheric Environment, 65, 177–185, https://doi.org/10.1016/j.atmosenv.2012.10.049, 2013.

Pinder, R. W., Gilliland, A. B. and Dennis, R. L.: Environmental impact of atmospheric $NH_3$ emissions under present and future conditions in the eastern United States, Geophysical Research Letters, 35(12), 89-90, doi:10.1029/2008GL033732, 2008.

Pu, W., Ma, Z., Collett, J. L., Guo, H., Lin, W., Cheng, Y., Quan, W., Li, Y., Dong, F. and He, D.: Regional transport and urban emissions are important ammonia contributors in Beijing, China, Environmental Pollution, 265, doi:10.1016/j.envpol.2020.115062, 2020.

Reay, D. S., Dentener, F., Smith, P., Grace, J. and Feely, R. A.: Global nitrogen deposition and carbon sinks, Nature Geoscience, 1(7), 430-437, doi:10.1038/ngeo230, 2008.

Saraswati, George, M. P., Sharma, S. K., Mandal, T. K. and Kotnala, R. K.: Simultaneous Measurements of Ambient NH 3 and Its Relationship with Other Trace Gases, $PM_{2.5}$ and Meteorological Parameters over Delhi, India, Mapan - Journal of Metrology Society of India, 34(1), 55–69, doi:10.1007/s12647-018-0286-0, 2019.

Singh, S. and Kulshrestha, U. C.: Rural versus urban gaseous inorganic reactive nitrogen in the Indo-Gangetic plains (IGP) of India, Environ. Res. Lett., 9(12), 125004, https://doi.org/10.1088/1748-9326/9/12/125004, 2014.

Teng, X., Hu, Q., Zhang, L., Qi, J., Shi, J., Xie, H., Gao, H. and Yao, X.: Identification of Major Sources of Atmospheric $NH_3$ in an Urban Environment in Northern China during Wintertime, Environmental Science and Technology, 51(12), 6839-6848, doi:10.1021/acs.est.7b00328, 2017.

UN Environment 2019. A Review of 20 Years' Air Pollution Control in Beijing. United Nations Environment Programme, Nairobi, Kenya. https://www.unenvironment.org/resources/report/review-20-years-air-pollution-control-beijing.

Vogt, E., Held, A. and Klemm, O.: Sources and concentrations of gaseous and particulate reduced nitrogen in the city of Münster (Germany), Atmospheric Environment, 39(38), 7393–7402, https://doi.org/10.1016/j.atmosenv.2005.09.012, 2005.

Wang, K., Fan, S., Guo, J. and Sun, G.: Characteristics of ammonia emission from motor vehicle exhaust in Beijing, Environmental Engineering, 36(03), 98–101, doi:10.13205/j.hjgc.201803020, 2019.

Warner, J. X., Dickerson, R. R., Wei, Z., Strow, L. L., Wang, Y. and Liang, Q.: Increased atmospheric ammonia over the world's major agricultural areas detected from space, Geophysical Research Letters, 44(6), 2875–2884, doi:10.1002/2016GL072305, 2017.

Wei, S., Dai, Y., Liu, B., Zhu, A., Duan, Q., Wu, L., Ji, D., Ye, A., Yuan, H., Zhang, Q., Chen, D., Chen, M., Chu, J., Dou, Y., Guo, J., Li, H., Li, J., Liang, L., Liang, X., Liu, H., Liu, S., Miao, C. and Zhang, Y.: A China data set of soil properties for land surface modeling, Journal of Advances in Modeling Earth Systems, 5(2), 212–224, doi:10.1002/jame.20026, 2013.

Wentworth, G. R., Murphy, J. G., Benedict, K. B., Bangs, E. J. and Collett, J. L.: The role of dew as a night-time reservoir and morning source for atmospheric ammonia, Atmospheric Chemistry and Physics, 16(11), 7435–7449, doi:10.5194/acp-16-7435-2016, 2016.

Wu, Z., Hu, M., Shao, K. and Slanina, J.: Acidic gases, NH3 and secondary inorganic ions in $PM_{10}$ during summertime in Beijing, China and their relation to air mass history, Chemosphere, 76(8), doi:10.1016/j.chemosphere.2009.04.066, 2009.

Zhang, B.: Atmospheric Distribution and Variation of $NH_3$ in Beijing, Environmental Science and Management 41(01), 119–122, 2016.

Zhang, S., Wag, A., Zhang, Z., Wang, J., Han, Y., Su, R. and Qu, Y.: On creating an anthropogenic ammonia emission inventory in capital Beijing, Journal of Safety and Environment, 16(02), 242–245, doi:10.13637/j.issn.1009–6094.2016.02.047, 2016.

Zhang, X., Wu, Y., Liu, X., Reis, S., Jin, J., Dragosits, U., van Damme, M., Clarisse, L., Whitburn, S., Coheur, P. F. and Gu, B.: Ammonia emissions may be substantially underestimated in China, Environmental Science and Technology, 51(21), 12089–12096, doi:10.1021/acs.est.7b02171, 2017.

Zhang, Y., Tang, A., Wang, D., Wang, Q., Benedict, K., Zhang, L., Liu, D., Li, Y., Collett Jr., J. L., Sun, Y. and Liu, X.: The vertical variability of ammonia in urban Beijing, China, Atmospheric Chemistry and Physics, 18(22), 16385–16398, doi:10.5194/acp-18-16385-2018, 2018.

Zhao, X., Xie, Y. X., Xiong, Z. Q., Yan, X. Y., Xing, G. X. and Zhu, Z. L.: Nitrogen fate and environmental consequence in paddy soil under rice-wheat rotation in the Taihu lake region, China, Plant and Soil, 319(1), 225-234, doi:10.1007/s11104-008-9865-0, 2009.

Zhou, C., Zhou, H., Holsen, T. M., Hopke, P. K., Edgerton, E. S. and Schwab, J. J.: Ambient Ammonia Concentrations Across New York State, Journal of Geophysical Research: Atmospheres, 124(14), 8287–8302, doi:10.1029/2019JD030380, 2019.